Journal of Thermal Science Vol.33, No.4 (2024) 1480−1490

**https://doi.org/10.1007/s11630-024-1997-x** **Article ID: 1003-2169(2024)04-1480-11**

# An Improved Thermal Conductivity Measurement Scheme for Macroscopic Graphitic Films Using the Laser Flash Method

**ZHANG Peijuan[1#], MING Xin[1#], LIU Yingjun[1,2*], WANG Xuelong[1], SHI Hang[1], HAO Yuanyuan[1], LU Jiahao[1], LIU Zheng[3], LAI Haiwen[4], ZHANG Ying[5], GAO Weiwei[1,2], XU Zhen[1,2], GAO Chao[1,2*]**

1. MOE Key Laboratory of Macromolecular Synthesis and Functionalization, Department of Polymer Science and Engineering, Key Laboratory of Adsorption and Separation Materials & Technologies of Zhejiang Province, Zhejiang University, Hangzhou 310027, China
2. Shanxi-Zheda Institute of Advanced Materials and Chemical Engineering, Taiyuan 030032, China
3. Special Equipment Safety Supervision and Inspection Institute of Jiangsu Province, National Graphene Products Quality Inspection and Testing Center (Jiangsu), Wuxi 214174, China
4. Hangzhou Gaoxi Technol Co., Ltd, Hangzhou 311113, China
5. China Academy of Aerospace Aerodynamics, Beijing 100074, China



**Abstract:** Achieving efficient thermal management urges to exploit high-thermal-conductivity materials to satisfy the boosted demand of heat dissipation. It is critical to adopt standardized characterization protocols to evaluate the intrinsic thermal conductivity of thermal management materials. However, for the most representative laser flash method, the lack of standard measurement methodology and systematic description on the thermal diffusivity and influencing factors has led to significant deviations and confusion of the thermal conduction performance in the emerging thermal management application. Here, the measurement error factors of thermal diffusivity by the common laser flash analyzer (LFA) are discussed. Taking high-thermal-conductivity graphitic film (GF) as a typical case, the key factors are analyzed to guide the measurement protocol of related carbon-based thermal management materials. The basic principle of the LFA measurement, actual pre-processing conditions, instrument parameters setting, and data analysis are elaborated for accurate measurements. Furthermore, the graphene thick films and common isotropic materials are also extended to meet various thermal measurement requirements. Based on the existing practical problems, we propose a feasible test flow to achieve a unified and standardized thermal conductivity measurement, which is beneficial to the rapid development of carbon-based thermal management materials.

**Keywords: thermal management; graphitic film; laser flash method; thermal conductivity; thermal diffusivity**

# ZHANG Peijuan and MING Xin contributed equally to this work.

Received: Sep 01, 2023 AE: MA Weigang

Corresponding author: LIU Yingjun; GAO Chao

E-mail: yingjunliu@zju.edu.cn chaogao@zju.edu.cn

## 1. Introduction

The miniaturized and integrated electronic devices have reached a staggering power density with $10^3$ W/cm$^2$ [1, 2] (Fig. 1(a)). The ensuing thermal management technology has become an important research topic in the past decades (Fig. 1(b)). Owing to the ultra-high thermal conductivity, flexibility, low-cost, lightweight, and easy-processable advantages, the graphitic materials have tremendous potential to achieve effective thermal management [3–5]. In recent years, most efforts have been paid to improve the thermal conduction performance of graphitic thermal management materials [5–15]. However, it is difficult and confusing to correctly evaluate and compare the reported thermal conductivity of graphitic films in different measurement conditions [16, 17].

As the most common thermal conductivity measurement instrument, the LFA features wide measuring range, easy operation, and time-saving than other methods, in which the thermal diffusivity is obtained by a function of the half-time $t_{0.5}$ from the flash pulse heating to the time where the back surface temperature reaches half of its maximum. This laser flash method was first described by Parker et al., which could obtain the cross-plane thermal property by involving collected temperature curve (Fig. 1(g)) [18]. Then, Donaldson measured in-plane thermal diffusivity by

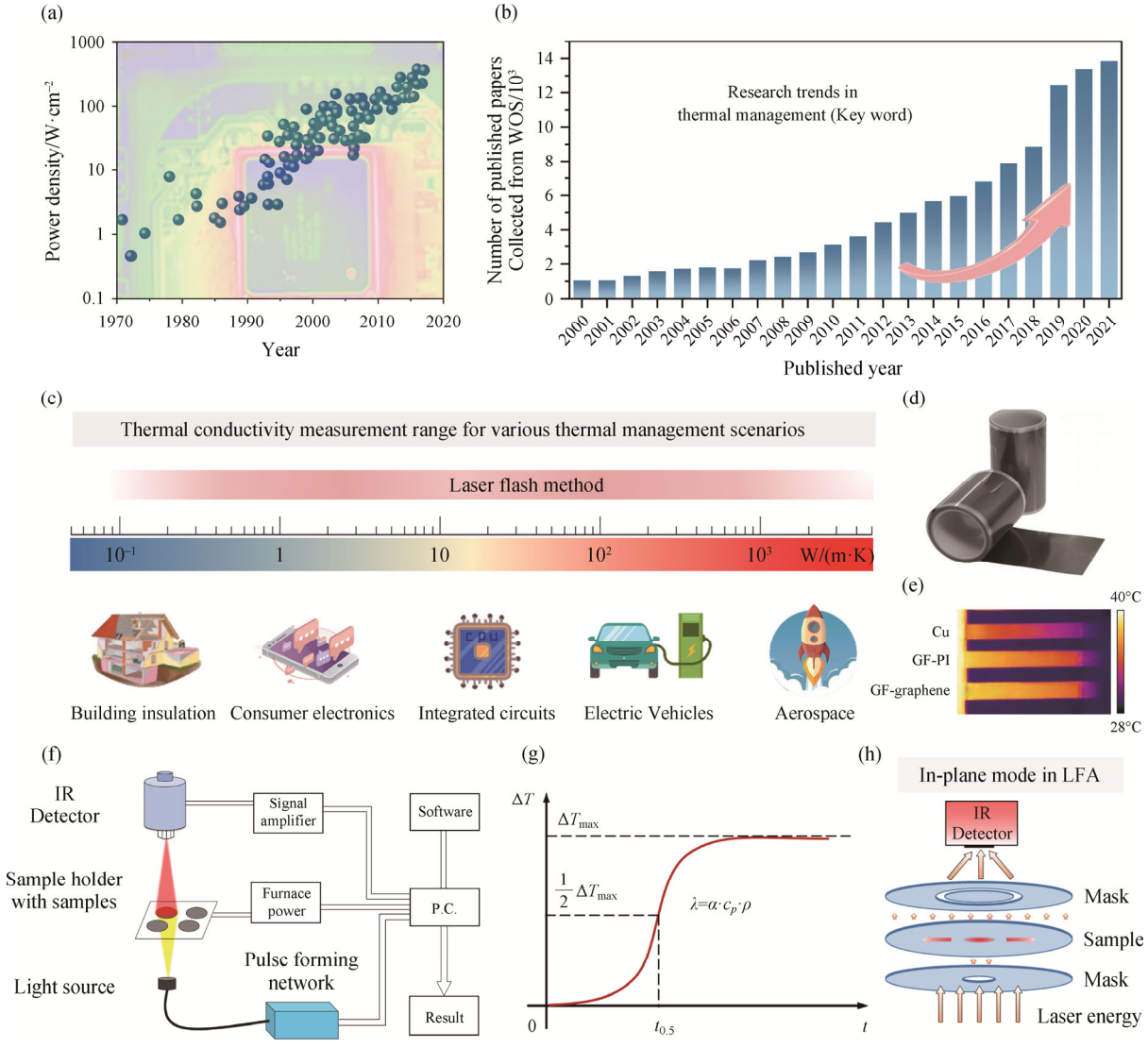


**Fig. 1** The trend of (a) power density of commercial processors and (b) the number of research articles in the thermal management field over the last decades. (c) The thermal conductivity measurement range of the laser flash method for various thermal management scenarios. (d) Digital images of large-area high-thermal-conductivity graphitic films. (e) Infrared image of Cu foil, GF-PI, and GF-graphene. (f) Principle of thermal diffusivity measurement by the laser flash method. (g) Ideal temperature curve detected from the back of sample. (h) Schematic diagram of in-plane thermal diffusivity measurement by the LFA.

pulse heating the center of the sample and measured the temperature rise at fixed intervals in the in-plane direction. At present, the LFA can measure materials with different thermal conductivity from 0.1 to 2000 W/(m·K), used in building insulation, consumer electronics, integrated chips, electric vehicles, and aerospace (Fig. 1(c)) [19]. However, regarding using the LFA to measure the thermal conductivity of graphitic film (GF), the sample pre-treatment and actual testing conditions have significant impacts on the testing results, such as the graphite coating effect [20], finite pulse time effect [21], radiant heat loss effect [22], and the temperature-dependent nature of carbon materials [23], etc., rendering it challenging to acquire credible value. The lack of measurement specification of the whole process severely limits the objective understanding of the thermal conduction behavior about the emerging thermal management materials.

Here, we have discussed the reliable measurement and general error analysis of in-plane thermal diffusivity by the LFA. For the high-thermal-conductivity GF, the widely used film material, the key measurement factors are summarized to guide the protocol of related carbon-based thermal management materials (Fig. 1(d)–(e)). We have deeply understood and generalized the accurate LFA measurement from four aspects, including the basic principle of the LFA measurement, actual pre-processing conditions, instrument parameter setting, and data analysis. To meet the booming thermal management requirements, the in-plane thermal conductivity measurement methods for graphene thick films and isotropic materials are also discussed and extended. We hope this work could help the community to achieve a consistent evaluation of the thermal conduction performances of carbon-based materials, laying down a solid foundation for sustainable development of carbon-based thermal management.

## 2. Experimental Section

Thermal conductivity of all samples were measured in a NETZSCH LFA 467 HyperFlash instrument by laser flash method. The test samples were firstly cut into round shapes with a diameter of 25.4 mm in in-plane mode, and square with sides of length 10 mm in cross-plane mode (vertical direction). Then, we can obtain thermal diffusivity, which was the average of three measurements. Each measurement was carried out after 30 minutes of turning on the instrument and adding liquid nitrogen to ensure the infrared detector and the instrument were in a stable state during each measurement.

Finally, the thermal conductivity ($K$) was calculated according to the following equation:

$$K = \rho \cdot C_p \cdot \alpha \tag{1}$$

In Eq. (1), $\rho$ is the density; $C_p$ is the specific heat, and $\alpha$ is the thermal diffusivity from LFA.

Experimental materials and any characterizations are available in the Supporting Information.

## 3. Results and Discussion

### 3.1 Principles of laser flash method

The laser flash method was firstly described by Parker et al. [24], involving heating the sample front by a preset pulse laser and measuring the temperature response of the sample back by an infrared detector (Fig. 1(f)). Thermal diffusivity can be calculated from the collected temperature curve. Then, the thermal conductivity is obtained by multiplying the thermal diffusivity, density, and specific heat capacity of the sample (Fig. 1(g)). Similarly, Donaldson measured the in-plane thermal diffusivity of Armco iron by pulse heating the center and measuring the radial temperature of the sample through the same testing process [25, 26]. With the continuous development of 2D anisotropic materials, a new measurement mode is developed to measure the in-plane thermal conductivity of thin films and anisotropic materials (Fig. 1(h)).

More specifically, the physical model of the laser flash method specifies the following assumptions [27]. (a) The sample is ideally non-transparent, thermally insulated, and homogeneous. (b) The thermophysical properties and density of the sample are constant when applying the pulsed laser to induce the temperature shift. (c) The laser pulses are extremely short compared with the temperature rise time of the sample. (d) The intensity of the laser beam spot is uniform and the laser energy is fully absorbed by the sample front. (e) The heat transfer process follows a one-dimensional heat transfer model throughout the expected $x$ direction with no heat losses.

Hence, the temperature at a given time $T(x,t)$ on the back surface of the sample ($x=h$) could be calculated by the following expression [24]:

$$T(h,t) = \frac{Q}{\rho C_p h}\left[1 + 2\sum_{n=1}^{\infty}\left(-1^n\right)\exp\left(\frac{-n^2\pi^2\alpha t}{h^2}\right)\right] \tag{2}$$

where $t$ is time; $h$ is the sample thickness; $Q$ is the impulse energy per unit surface area; $\rho$, $C_p$, and $\alpha$ are the density, specific heat capacity, and thermal diffusivity, respectively. Then, two dimensionless parameters are defined, including normalized back surface temperature:

$$T_{\mathrm{N}}(h,t) = \frac{T(h,t)}{T_{\max}} \tag{3}$$

and dimensionless time:

$$\omega = \frac{\pi^2\alpha t}{h^2} \tag{4}$$

where $T_{max}$ represents the maximum temperature at the back surface after a pulse. Using Eqs. (2), (3), and (4), the following equation can be obtained:

$$T(h,t)=1+2\sum_{n=1}^{\infty}\left(-1^{n}\right)\exp\left(-n^{2}\omega\right) \tag{5}$$

The thermal diffusivity could be obtained by assessing the situation where the back surface temperature has reached half of the maximum value ($V$=0.5) (Fig. 1(g)). In this case, the corresponding dimensionless time $\omega$ is 1.38. From the expression of Eq. (4), the cross-plane thermal diffusivity could then be expressed as:

$$\alpha=\frac{1.38h^{2}}{\pi^{2}t_{0.5}} \tag{6}$$

Then, Donaldson and Heckmanto extended a mathematical solution for the measurement of in-plane thermal diffusivity [25, 26]. In this method, the thermal diffusivity in the radial direction is calculated below [28]:

$$\alpha=\frac{R^{2}\tau_{0.5}}{t_{0.5}} \tag{7}$$

where $R$ is the pulse radius; $\tau_{0.5}$ is a computed Fourier number corresponding to a fractional temperature ratio of 50%, which is determined for appropriate values of $\sigma$ ($\sigma$ =$r$/$R$; $r$ is the radial heat transfer distance). The $t_{0.5}$ is the time when the temperature at radius $r$ rises to half-maximum.

With the continuous development of high thermal conductivity thin films, the traditional cross-plane mode gradually becomes inapplicable, due to the temperature rise time of this sample being too short to be effectively identified by LFA. Therefore, according to the research of Donaldson and Heckmanto above, the laser flash method developed an in-plane measurement mode to measure the thermal conductivity of thin films and anisotropic materials. In this mode, in-plane thermal diffusivity could be obtained by pulse heating the center of the sample, and measuring the temperature rise at fixed intervals in the in-plane direction (Fig. 1(h)), which is different from the heat transfer direction of the cross-plane physical model and separates the heat transfer path from the thickness direction.

Eqs. (6) and (7) provide a simplified method for determining the thermal diffusivity of an unknown sample by precisely measuring the $t_{0.5}$. Therefore, experimental measurements should be controlled to closely fit the presupposition, so as to obtain precise $t_{0.5}$ through the temperature curve from the LFA.

### 3.2 Pre-processing conditions and processes

The samples should be prepared to follow the standard mold size with a diameter of 25.4 mm for in-plane mode. The surface of the sample should be smooth. Unmatched sizes and damaged surfaces would influence the testing accuracy. Here, we utilize the high-thermal-conductivity GF as a typical case to specify influencing factors in testing to standardize the measurement process. The LFA is in the normal operating condition. Except for the study of specific variables, all measurement processes are based on the recommended measurement specifications of this paper. The temperature response is derived from the absorbed laser energy, which is subsequently detected by an infrared temperature sensor. Thus, for an adequate signal response, the pulse absorption and infrared emissivity of the sample surface should be considered. Applying the graphite coating to both surfaces of samples is regular to improve signal amplitude as a traditional pre-treatment method, particularly for reflective samples (Fig. S1 and Fig. S2). Graphite coating could unify the infrared emissivity of different materials and improve its absorption to over 90% (Fig. 2(a)), and effectively enhance the signal intensity of temperature rise to nearly double times (Fig. 2(e)), thus avoiding errors caused by infrared temperature measurements.

In this regard, the uniformity of graphite coating could increase the surface roughness of the sample by more than 20% (Fig. 2(b)–(d) and Fig. S3). This will potentially increase the unevenness of the measurements, especially for the cross-plane mode with the requisite plane parallelism. Additionally, excessive graphite coating may significantly underestimate the results [20]. Our results for the GF show that excessive graphite coating leads to a significant thermal conductivity reduction of about 50% (Fig. 2(e), Fig. S4, and Table S2). This performance degradation could be attributed to the thermal resistance introduced by the overmuch graphite coating layer (thermal resistance of graphite layer and the contact resistance between the graphite layer and the sample surface) (Fig. S5), which should not be disregarded on the other similar thin-film samples with high thermal conductivity [20, 29, 30]. A number of studies have been made to resolve the error caused by the graphite coating on the sample surface. Various theories have been presented to predict the thermal resistance of the graphite coating [31–34], yet the majority of that is not in good agreement with the experimental data. Therefore, we propose a modified graphite coating method with better practical availability. As a modified pre-treatment method, it is recommended to coat the areas subject to laser and infrared detection only (Fig. 2(f)), which could improve the laser absorption while minimizing the adverse thermal resistance effects of graphite coating. Compared with the traditional pre-treatment with entire graphite coating, the thermal conductivity of GFs using the modified graphite coating method shows an improvement of approximately 30% (Fig. 2(g)–(h) and Table S3). As another classic case, the thermal conductivity of pure copper closely agrees with

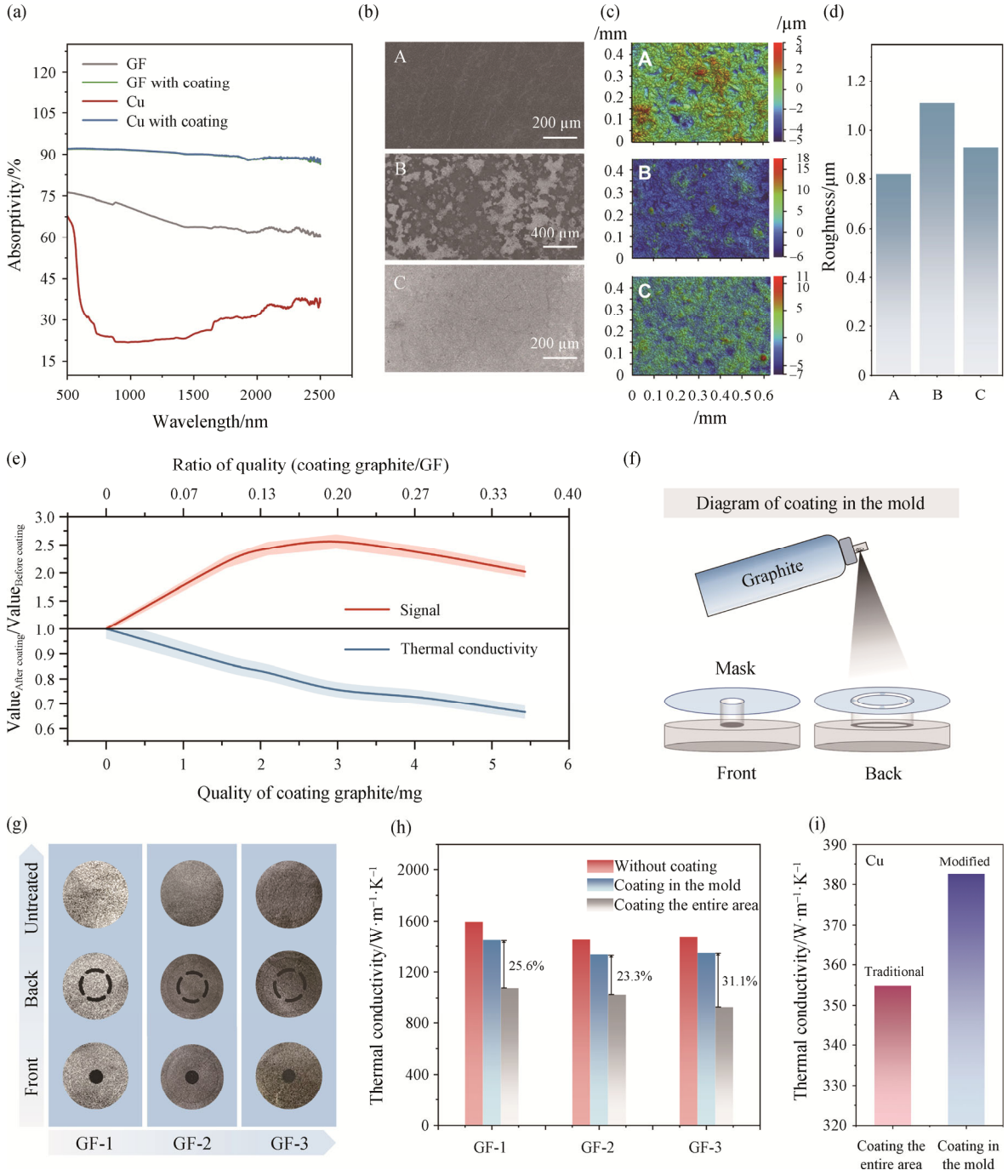


**Fig. 2** (a) Absorptivity of different samples before and after graphite coating. (b) SEM images of different graphite coating states. (c) Stereoscopic images and (d) roughness of different graphite coating states from optical profilometer. The three coating states are as follows: A: without coating, B: incomplete coating, C: complete coating. (e) Influence of graphite coating quality on infrared detector signals and measurement results. (f) Diagram of modified graphite coating. (g) Digital images of three kinds of GFs before and after modified graphite coating. (h) Measurement results of different pre-treatment methods for three kinds of GFs. (i) Measurement results of different pre-treatment methods for pure copper.

its theoretical value through this modified pre-treatment method (Fig. 2(i) and Fig. S6). These results indicate the importance of pre-treatments of the sample and the validity of the modified graphite coating method, which lays a solid foundation for subsequent measurements.

### 3.3 Parameters setting and data analysis

Appropriate parameters should be set for an accurate $t_{0.5}$ from the well-shape temperature-response curve, including the impulse voltage, pulse width, and the fitted model (Fig. 3(a)). The correct temperature-response

curve requires appropriate signal amplitude, good signal-to-noise ratio, and no obvious interference between the pulse signal and the heat transfer signal so as to realize that the fitted curve is consistent with the actual temperature-response curve.

Concretely, the impulse voltage and pulse width determine the laser energy which affects the output signal to generate different results for the same sample [35]. As shown in Fig. 3(b), higher energy input exactly lowers the measured thermal conductivity of GF, due to the excessive temperature rise which should not be ignored for the materials with temperature-dependent thermal conduction properties. An extrapolation method is expected to eliminate discrepancies caused by parameter differences [23, 36–38]. By obtaining a series of equivalent thermal conductivity at different temperature rises through changing the pulse energy, the intrinsic thermal conductivity of GF at zero-energy input state could be acquired by reasonable fitting extrapolation method (Fig. 3(c)). However, too weak laser energy would cause the signal curve with a poor signal-to-noise ratio, which is difficult to obtain effective measurement results with low coefficient of variation (<5%) (Fig. 3(d)–(e)). According to our statistical analysis, it's recommended that the signal amplitude should not be less than 4 times the noise fluctuation to realize high reliability (Tables S4–S6).

Meanwhile, the matching degree between the fitted temperature curve and the actual curve will also affect the accuracy of the results. Controlling the pulse time and adopting the pulse correction model are also crucial to avoid the impact of the finite pulse effect and the error of $t_{0.5}$ [39, 40]. As shown in Fig. 3(f), when the pulse width is too wide, such as 800 μs, there is a significant deviation between the response signal and the fitted curve with heat loss, resulting in the distortion between the fitted $t_{0.5}$ and the actual $t_{0.5}$. In addition, due to the temperature difference during measurement, there is an unavoidable heat loss between the sample and the surrounding environment [22, 39, 41]. Take the impulse voltage of 260 V and the pulse width of 40 μs as a test case, the actual temperature curve does not remain constant as the ideal model but decreases with time after reaching the maximum value (Fig. 3(g) and Table S7). We compared the results of two fitted models with or without adding heat loss, and there is a 5%–10% deviation between them (Fig. 3(h) and Table S8). Therefore, the heat loss should be considered in the mathematical fitted model to match reality.

### 3.4 Measurement of high-thermal-conductivity graphene films with thick thickness

Recently, the thickness of the carbon-based film gradually increases to meet the demand of heat dissipation at high heat flux density. Conventional polyimide-based films cannot be synthesized over hundred microns due to the restriction of molecular structural transformation in the complicated production process [42]. Thus, the available graphene film has become a new class of carbon-based films with high thermal conductivity due to its advantages of easy assembly into thick films, which has aroused great interest [7, 12]. How to accurately and easily characterize the thermal conductivity of graphene thick film is the fundamental issue in promoting its practical application. By measuring the thermal conductivity of graphene films with different thicknesses in the in-plane mode of LFA, it is found that the thermal conductivity decreases with the increment of thickness (Fig. 4(a)). We used another standard steady-state heat flow method to verify whether this degradation trend is repeatable. We found when the film thicknesses were above 150 μm, the difference in measured thermal conductivity could exceed 400 W/(m·K) (>30%). This could be attributed to the fact that in the in-plane mode of LFA measurement, heat conduction occurs in both in-plane and across-plane directions as the thickness of the graphene film increases (Fig. 4(b)) [25, 43]. This heat transfer pattern violates the assumption of one-dimensional heat transfer, which makes it difficult for the mathematical model of in-plane mode in the subsequent LFA test to correct this deviation. In this case, the "Laminate" mode in the LFA is recommended for the samples with thicknesses above 150 μm. The measured results are close to those obtained by the standard steady-state heat flow method (Fig. 4(a)). Specifically, the thick films were firstly cut into a rectangular with a long side ($L$) of 12.7 mm and the same height ($H$).

Subsequently, the thick samples are rotated 90° to make the direction of thickness turn from the $z$-axis to the $x$-axis and tightly stacked onto the mold until the total thickness approaches the length range of the mold (~ 10–15 mm) (Fig. 4(c) and Figs. S7–S8). The thermal conductivity of graphene thick films obtained via this method aligned well with those by the steady-state heat flow method (Fig. 4(a)). It exhibits consistent results by varying test heights (Fig. 4(d)), indicating the feasibility and accuracy of this flipping method for graphene thick films.

### 3.5 Measurement recommendations of various isotropic materials

Apart from emerging 2D anisotropic materials, various isotropic materials have a large proportion of applications in various heat dissipation scenarios, whose thermal conductivity varies greatly from ~0.24 of polymers to ~380 W/(m·K) of copper (Fig. 5(a)). It is important to realize the universal and standardized measurement process for LFA-based thermal conductivity.

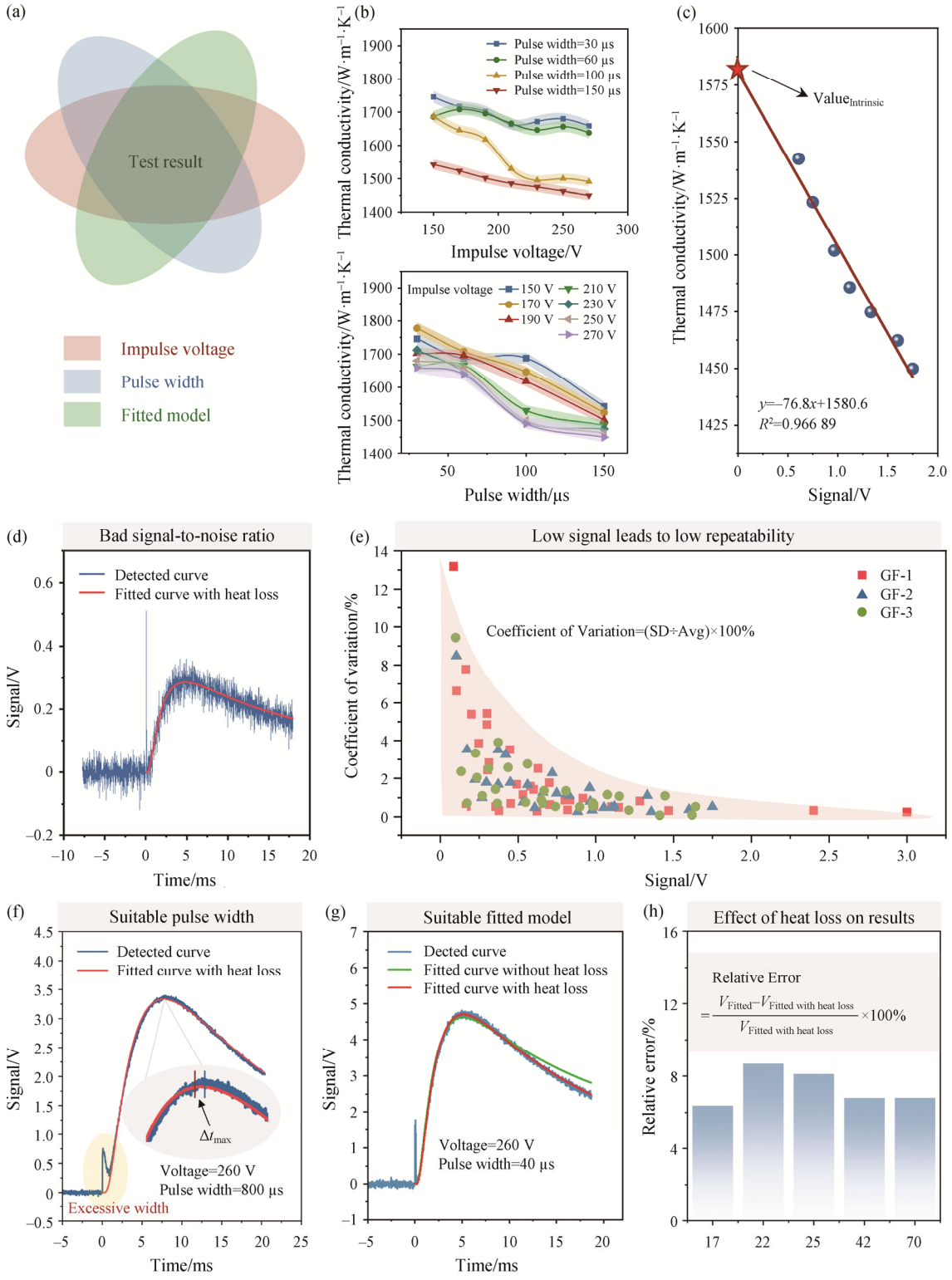


**Fig. 3** (a) Parameters that influence the test results from the LFA. (b) Thermal conductivity of the same sample under different impulse voltage and pulse width. (c) Thermal conductivity as a function of laser pulse energy. The horizontal axis represents the output signal of the infrared detector which is used to represent the laser pulse energy; an intrinsic thermal diffusivity is determined by extrapolation to the zero signal along this line. (d) Temperature curve with poor signal-to-noise ratio. (e) Coefficient of variation of measurement results under different output signals, whose value reflects the repeatability of measurement. (f) Temperature curve with significant overlap between the pulse peak and temperature rise curve, whose fitted curve does not match the actual curve, resulting in an error of $t_{0.5}$. (g) Temperature curve of the fitted model with or without heat loss. (h) Relative error of whether the fitted model counts heat loss or not. Pulse correction models were added to all the above fitted curves.

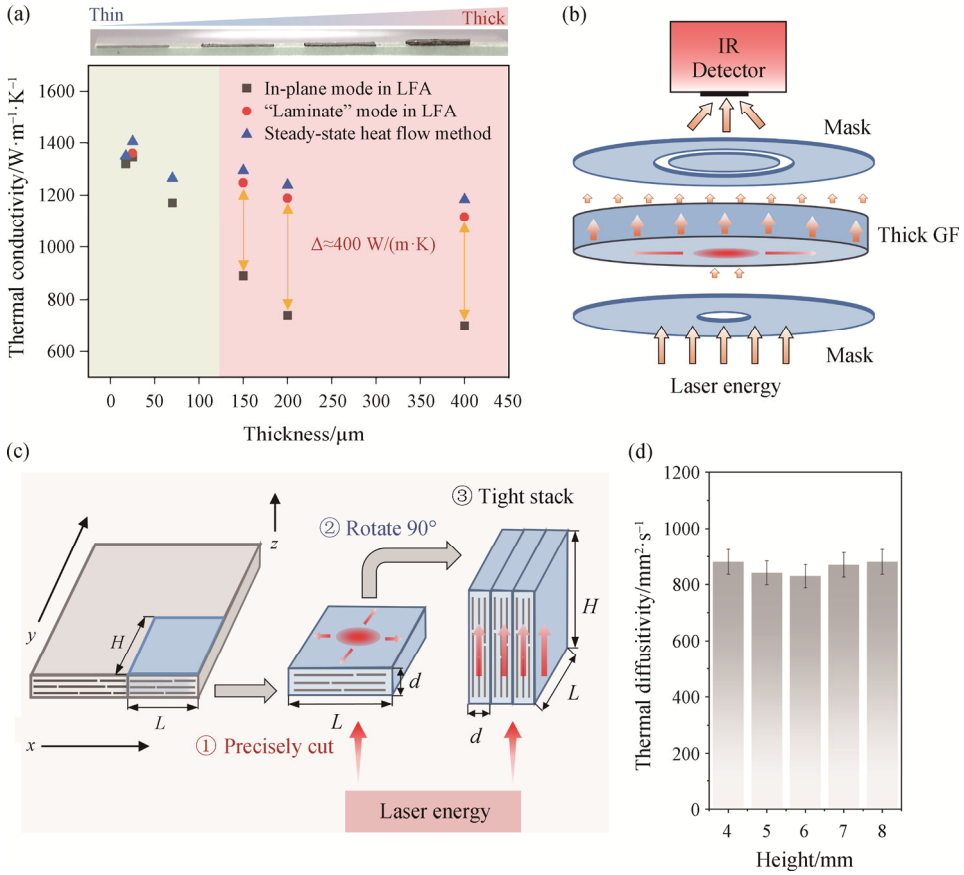


**Fig. 4** (a) Thermal conductivity of GFs at different thicknesses under different measurement methods. (b) Heat transport of thick films occurs in both in-plane and cross-plane directions. (c) Schematic diagram of measurement by "Laminate" mode. (d) Thermal conductivity of the same sample at different heights by "Laminate" mode in the LFA.

As mentioned in section 2.4, it's essential to select a suitable thickness range for accurate measurement in in-plane mode. Various representative isotropic materials could obtain almost the same thermal conductivity under varying test thicknesses through the vertical mode (Fig. 5(b) and Table S9) [44]. Using the vertical mode measurements in the LFA as reference values, the appropriate thickness range of the isotropic materials in the in-plane mode is determined by using the intersection of the measured results in these two modes. The following are empirical suggestions for choosing the appropriate sample thickness using the in-plane measurement model (Fig. 5(c)–(g)). When considering the comprehensive influence of the pre-treatment process and parameter setting, it is suggested that the reasonable thickness of PTFE could be 1.6–2 mm with less than a 3% error band (Fig. 5(c)). Similarly, for 304 stainless steel and alumina ceramic, the recommended thickness range is 0.4–0.6 mm (Fig. 5(d)–(e)). For brass, a thickness range of 0.3–1.1 mm is recommended (Fig. 5(f)), while for copper, a thickness of 0.3–1.5 mm is considered optimal (Fig. 5(g)). When samples exhibit ultra-high thermal conductivity, it is advisable to use thinner samples (<150 μm) in in-plane measurement mode as previously stated (Fig. 4(a)). It is recommended to use thinner thickness of samples with higher thermal conductivity (>100 W/(m·K)), which is also in accord with the original principles of in-plane mode development. For samples with low thermal conductivity (<30 W/(m·K)), it is recommended to use cross-plane mode to get a lower error (Fig. 5(h)).

## 4. Conclusion

The thermal conductivity measurement utilizing the laser flash method is frequently impacted by numerous variables, rendering it challenging to acquire dependable value. In this work, the influence factors of the thermal conductivity measurement for high-thermal-conductivity GF by the LFA are analyzed. Based on the comparison and analysis of thermal conductivity under different measurement conditions, we provide operational suggestions and standardized practical procedures to minimize the measurement error, so as to accurately reflect the inherent thermal transport properties of materials. Modified pre-treatment methods, suitable test parameters, and fitted models should be selected

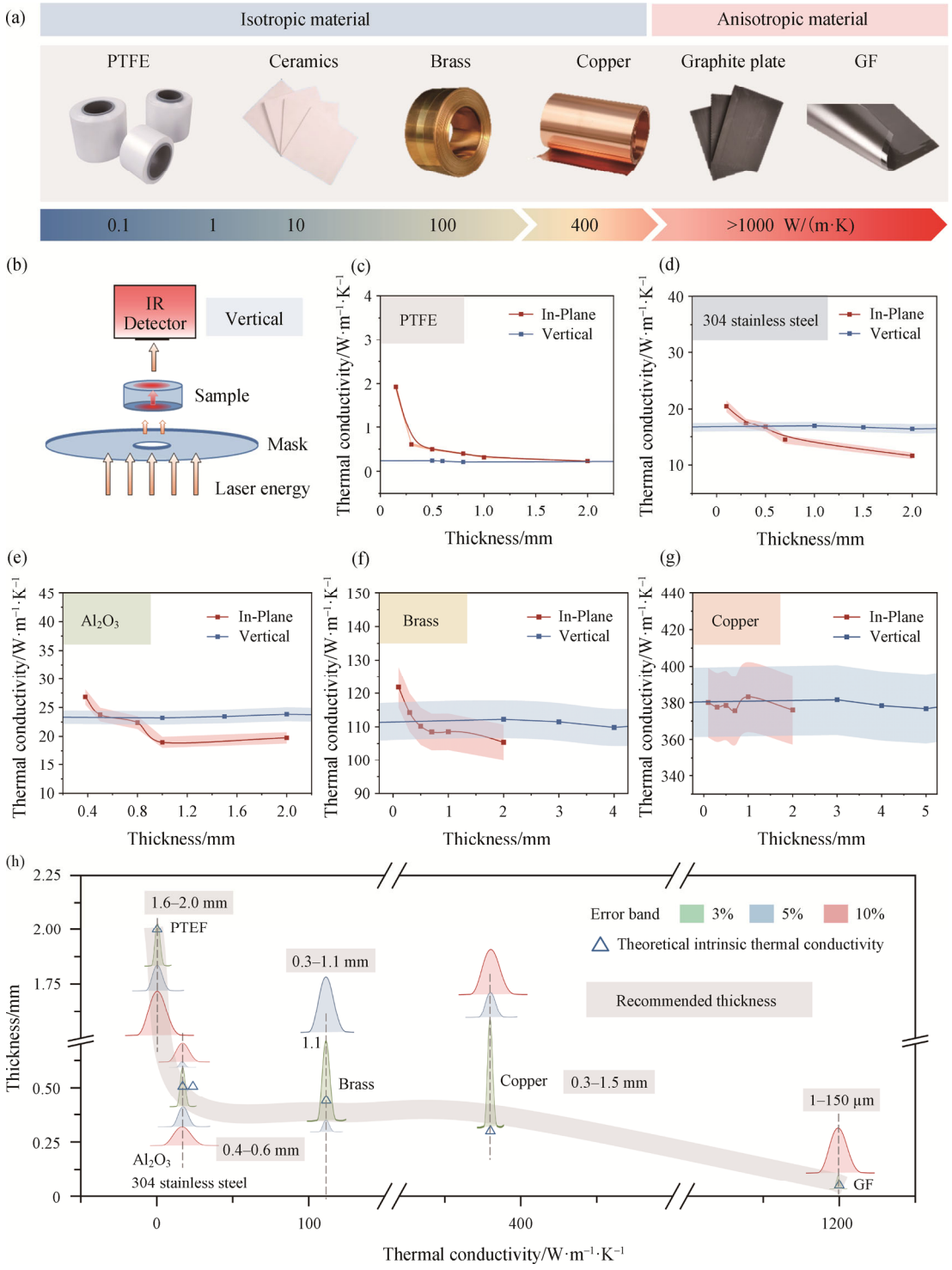


**Fig. 5** (a) The corresponding thermal conductivity of different materials. (b) Schematic diagram of thermal diffusivity measurement by vertical mode in the LFA. Measurements of thermal conductivity of isotropic materials in in-plane and vertical mode with different thicknesses, including (c) PTFE, (d) 304 stainless steel, (e) $Al_2O_3$, (f) brass, and (g) copper. (h) Recommended thickness for different thermal conductivity materials in in-plane mode measurements.

as suggested in this paper. Appropriate measurement schemes for in-plane thermal conductivity of fast-developing graphene thick films and common isotropic materials are also proposed. Through establishing a reliable thermal conductivity measurement protocol, we hope that this work will provide useful guidance for accurately reporting thermal conductivity in the field of thermal management.

## Acknowledgments

This work is supported by the National Natural Science Foundation of China (Nos. 52272046, 52090030, 52090031, 52122301, 51973191), the Natural Science Foundation of Zhejiang Province (LR23E020003), Shanxi-Zheda Institute of New Materials and Chemical Engineering (2021SZ-FR004, 2022SZ-TD011, 2022SZ-TD012, 2022SZ-TD014), Hundred Talents Program of Zhejiang University (188020*194231701/113, 112300+1944223R3/003, 112300+1944223R3/004), the Fundamental Research Funds for the Central Universities (Nos. 226-2023-00023, 226-2023-00082, 2021FZZX001-17, K20200060), National Key R&D Program of China (NO. 2022YFA1205300, NO. 2022YFA1205301, NO. 2020YFF0204400, NO. 2022YFF0609801), "Pioneer" and "Leading Goose" R&D Program of Zhejiang 2023C01190.

## Conflict of Interest

On behalf of all authors, the corresponding author states that there is no conflict of interest.

## Electronic Supplementary Materials

Supplementary materials are available in the online version of this article at

https://doi.org/10.1007/s11630-024-1997-x

## References

[1] Hamann H.F., Weger A., Lacey J.A., et al., Hotspot-limited microprocessors: Direct temperature and power distribution measurements. IEEE Journal of Solid-State Circuits, 2007, 42(1): 56–65.

[2] Smoyer J.L., Norris P.M., Brief historical perspective in thermal management and the shift toward management at the nanoscale. Heat Transfer Engineering, 2018, 40(3–4): 269–282.

[3] Wang F., Fang W., Ming X., et al., A review on graphene oxide: 2D colloidal molecule, fluid physics, and macroscopic materials. Applied Physics Reviews, 2023, 10(1): 011311.

[4] Ming X., Wei A., Liu Y., et al., 2D-topology-seeded graphitization for highly thermally conductive carbon fibers. Advanced Materials, 2022, 34(28): e2201867.

[5] Peng L., Xu Z., Liu Z., et al., Ultrahigh thermal conductive yet superflexible graphene films. Advanced Materials, 2017, 29(27): 1700589.

[6] Zhong J., Sun W., Wei Q., et al., Efficient and scalable synthesis of highly aligned and compact two-dimensional nanosheet films with record performances. Nature Communications, 2018, 9(1): 3484.

[7] Zhang X., Guo Y., Liu Y., et al., Ultrathick and highly thermally conductive graphene films by self-fusion. Carbon, 2020, 167: 249–255.

[8] Feng C.P., Wei F., Sun K.Y., et al., Emerging flexible thermally conductive films: mechanism, fabrication, application. Nano-Micro Letters, 2022, 14(1): 127.

[9] Xin G., Sun H., Hu T., et al., Large-area freestanding graphene paper for superior thermal management. Advanced Materials, 2014, 26(26): 4521–4526.

[10] Dai W., Ma T., Yan Q., et al., Metal-level thermally conductive yet soft graphene thermal interface materials. ACS Nano, 2019, 13(10): 11561–11571.

[11] Han Z., Wang J., Liu S., et al., Electrospinning of neat graphene nanofibers. Advanced Fiber Materials, 2021, 4(2): 268–279.

[12] Huang H., Ming X., Wang Y., et al., Polyacrylonitrile-derived thermally conductive graphite film via graphene template effect. Carbon, 2021, 180: 197–203.

[13] Dai W., Lv L., Lu J., et al., A paper-like inorganic thermal interface material composed of hierarchically structured graphene/silicon carbide nanorods. ACS Nano, 2019, 13: 1547–1554.

[14] Chen L., Liu T.H., Wang X., et al., Near-theoretical thermal conductivity silver nanoflakes as reinforcements in gap‐filling adhesives. Advanced Materials, 2023, 35(31): 2211100.

[15] Gao J., Yan Q., Lv L., et al., Lightweight thermal interface materials based on hierarchically structured graphene paper with superior through-plane thermal conductivity. Chemical Engineering Journal, 2021, 419: 129609.

[16] Kumar P., Shahzad F., Yu S., et al., Large-area reduced graphene oxide thin film with excellent thermal conductivity and electromagnetic interference shielding effectiveness. Carbon, 2015, 94: 494–500.

[17] Guo Y., Dun C., Xu J., et al., Ultrathin, washable, and large-area graphene papers for personal thermal management. Small, 2017, 13(44): 1702645.

[18] Palacios A., Cong L., Navarro M.E., et al., Thermal conductivity measurement techniques for characterizing thermal energy storage materials – A review. Renewable and Sustainable Energy Reviews, 2019, 108: 32–52.

[19] Group - NETZSCH Holding. https://www.netzsch.com/en.

[20] Kim S.K., Kim Y.J., Determination of apparent thickness of graphite coating in flash method. Thermochimica Acta, 2008, 468(1–2): 6–9.

[21] Cape J.A., Lehman G.W., Temperature and finite pulse-time effects in the flash method for measuring thermal diffusivity. Journal of Applied Physics, 1963, 34(7): 1909–1913.

[22] Cowan R.D., Pulse method of measuring thermal

diffusivity at high temperatures. Journal of Applied Physics, 1963, 34(4): 926–927.

[23] Akoshima M., Baba T., Study on a thermal-diffusivity standard for laser flash method measurements. International Journal of Thermophysics, 2006, 27(4): 1189–1203.

[24] Parker W.J., Jenkins R.J., Butler C.P., et al., Flash method of determining thermal diffusivity, heat capacity, and thermal conductivity. Journal of Applied Physics, 1961, 32(9): 1679–1684.

[25] Donaldson A.B., Radial conduction effects in the pulse method of measuring thermal diffusivity. Journal of Applied Physics, 1972, 43(10): 4226–4228.

[26] Donaldson A.B., Taylor R.E., Thermal diffusivity measurement by a radial heat flow method. Journal of Applied Physics, 1975, 46(10): 4584–4589.

[27] Vozár L., Hohenauer W., Flash method of measuring the thermal diffusivity. A review. High Temperatures-High Pressures, 2003, 35/36(3): 253–264.

[28] Chu F.I., Taylor R.E., Donaldson A.B., Thermal diffusivity measurements at high temperatures by the radial flash method. Journal of Applied Physics, 1980, 51(1): 336–341.

[29] Lim K.H., Kim S.K., Chung M.K., Improvement of the thermal diffusivity measurement of thin samples by the flash method. Thermochimica Acta, 2009, 494(1–2): 71–79.

[30] Liu Y., Qiu L., Liu J., et al., Enhancing thermal transport across diamond/graphene heterostructure interface. International Journal of Heat and Mass Transfer, 2023, 209: 124123.

[31] Qiu L., Ma Y., Wang S., et al., High-accuracy thermophysical property measurement technique based on Labview-3ω method. AIP Advances, 2023, 13(4): 045014.

[32] Cernuschi F., Lorenzoni L., Bianchi P., et al., The effects of sample surface treatments on laser flash thermal diffusivity measurements. Infrared Physics & Technology, 2002, 43(3–5): 133–138.

[33] Milošević N.D., Simultaneous estimation of the thermal diffusivity and thermal contact resistance of thin solid films and coatings using the two-dimensional flash method. International Journal of Thermophysics, 2003, 24(3): 799–819.

[34] Litovsky E., Horodetsky S., Kleiman J., Non-destructive thermal diagnostics of porous materials. International Journal of Thermophysics, 2005, 26(6): 1815–1831.

[35] Blumm J., Lemarchand S., Influence of test conditions on the accuracy of laser flash measurements. High Temperatures-High Pressures, 2002, 34(5): 523–528.

[36] Baba T., Ono A., Improvement of the laser flash method to reduce uncertainty in thermal diffusivity measurements. Measurement Science and Technology, 2001, 12(12): 2046–2057.

[37] Ohta H., Baba T., Shibata H., et al., Evaluation of the effective sample temperature in thermal diffusivity measurements using the laser flash method. International Journal of Thermophysics, 2002, 23(6): 1659–1668.

[38] Akoshima M., Hay B., Zhang J., et al., International comparison on thermal-diffusivity measurements for iron and isotropic graphite using the laser flash method in CCT-WG9. International Journal of Thermophysics, 2012, 34(5): 763–777.

[39] Cape J.A., Lehman G.W., Temperature and finite pulse‐time effects in the flash method for measuring thermal diffusivity. Journal of Applied Physics, 1963, 34(7): 1909–1913.

[40] Taylor R.E., Cape J.A., Finite pulse-time effects in the flash diffusivity technique. Applied Physics Letters, 1964, 5(10): 212–213.

[41] Cezairliyan A., Baba T., Taylor R., A high-temperature laser-pulse thermal diffusivity apparatus. International Journal of Thermophysics, 1994, 15(2): 317–341.

[42] Gouzman I., Grossman E., Verker R., et al., Advances in polyimide-based materials for space applications. Advanced Materials, 2019, 31(18): e1807738.

[43] Watt D.A., Theory of thermal diffusivity by pulse technique. British Journal of Applied Physics, 1966, 17(2): 231–240.

[44] Schoderböck P., Klocker H., Sigl L.S., et al., Evaluation of the thermal diffusivity of thin specimens from laser flash data. International Journal of Thermophysics, 2009, 30(2): 599–607.